

Multimagnetic Monopoles

D. Bazeia,¹ M. A. Liao,¹ and M. A. Marques²

¹*Departamento de Física, Universidade Federal da Paraíba, 58051-970 João Pessoa, PB, Brazil*

²*Departamento de Biotecnologia, Universidade Federal da Paraíba, 58051-900 João Pessoa, PB, Brazil*

(Dated: December 23, 2024)

In this work we investigate the presence of magnetic monopoles that engender multimagnetic structures, which arise from an appropriate extension of the $SU(2)$ gauge group. The investigation is based on a modified relativistic theory that contain several gauge and matter fields, leading to a Bogomol'nyi bound and thus to a first order framework, from which stable multimagnetic solutions can be constructed. We illustrate our findings with several examples of stable magnetic monopoles with multimagnetic properties.

I. INTRODUCTION

Magnetic monopole has been an important object of investigation in theoretical physics ever since Dirac first showed that it can be incorporated into the framework of electromagnetism in a simple and elegant way [1, 2]. Of particular importance is the demonstration, also given by Dirac, that their mere existence could, when combined with the postulates of quantum mechanics, provide a natural explanation for the quantization of electric (and magnetic) charge.

Despite this theoretical triumph, lack of experimental evidence for the existence of monopoles led Dirac's theory to be regarded as a mathematical curiosity. Almost fifty years later, 't Hooft [3] and Polyakov [4] independently found a topological monopole solution for a Yang-Mills-Higgs theory; see also Refs. [5–7]. The 't Hooft-Polyakov monopole presents a magnetic charge which is directly proportional to a topological invariant called the winding number, or topological degree [8, 9]. Perhaps even more important than the solution itself was the realization that magnetic monopoles were an unavoidable consequence of spontaneous symmetry breaking in grand unification theories [3]. The so called monopole problem, regarding the apparent absence of these particles in our universe despite the theoretical predictions of their production in the early universe [10] was one of the main motivations for the development of inflationary universe models [11, 12].

The study of magnetic monopoles has further evolved by the introduction of models with enhanced gauge symmetry [13, 14]. This enhancement allows for more complex monopoles, which now emerge from a much richer topology and present internal structure. Works [15–17] have been developed along these lines, and we have also conducted a similar investigation in $(2,1)$ dimensions, which led to vortices possessing a novel internal structure, which is reflected by the magnetic field associated with these solutions [18].

In this work we will build upon the investigation conducted in [17] to construct multimagnetic structures, which emerge from the superposition of magnetic shells, each of which is the result of spontaneous symmetry breaking in a $SU(2)$ subgroup of the full gauge group,

under whose transformations our models will be taken to be invariant. Research from the last decade has brought to light a great variety of interesting applications for bimagnetic structures, ranging from engineering to biomedicine [19–22]. One particularly interesting application lies in the possibility of using the exchange bias present on multilayers of magnetic material for beating the superparamagnetic limit, which normally constrains the miniaturization of magnetic recording devices [23, 24]. Such multilayered or onyon-like structures have been investigated in relation to nanoparticles [25, 26] and, as multimagnetic structures expand upon the bimagnetic models studied earlier, so we hope that the systems investigated here may be useful to expand on the aforementioned applications. Another interesting property of our models lie in the presence of a Bogomol'nyi-Prasad-Sommerfield (BPS) limit, in which the problem is reduced to the solution of a system of first order differential equations. Solutions of this type are global minima of the energy, and are therefore expected to be stable under small fluctuations.

Magnetic monopoles have also been found in spin ice systems [27, 28] and more recently, the direct observation of static and dynamics of emergent magnetic monopoles in a chiral magnet has been reported in Ref. [29]. They are also object of theoretical and experimental study in heavy-ion collisions and in neutron stars [30], and also in the international research collaboration MoEDAL running at CERN with the prime goal of searching for the magnetic monopole [31]. These studies motivate that we investigate new models of magnetic monopoles in high energy physics, hoping to contribute with the construction of models that allow the addition of internal structure, bringing novel properties and/or features at the fundamental level.

In order to disclose the investigation, we organize the present work as follows: In Sec. II we introduce the generalized Lagrangian that defines our models, and derive the second order equations that follow from it. We then investigate the conditions under which a Bogomol'nyi bound is attainable, and examine the first order equations which must be satisfied by BPS solutions. We then proceed, in Sec. III and IV, to solve some examples which engender the sought-after multimagnetic structures, and

investigate their properties. Finally, in Sec. V, we discuss our results and add some perspectives of future works in the subject.

II. GENERAL PROCEDURE

We work in four dimensional Minkowski spacetime with metric $(-, +, +, +)$, and consider a class of non-abelian models with the Lagrangian density of the form

$$\begin{aligned} \mathcal{L} = & - \sum_{n=1}^N \frac{P^{(n)}(\{|\phi|\})}{4} F_{\mu\nu}^{(n)a} F^{(n)a\mu\nu} \\ & - \sum_{n=1}^N \frac{M^{(n)}(\{|\phi|\})}{2} D_{\mu}^{(n)} \phi^{(n)a} D^{(n)\mu} \phi^{(n)a} \\ & - V(\{|\phi|\}), \end{aligned} \quad (1)$$

where N is a positive integer, $(\{|\phi|\})$ stands for the set $(|\phi^{(1)}|, |\phi^{(2)}|, \dots, |\phi^{(N)}|)$, $D_{\mu}^{(k)} \phi^{(k)a} = \partial_{\mu} \phi^{(k)a} + g^{(k)} \varepsilon^{abc} A_{\mu}^{(k)b} \phi^{(k)c}$ is the action of covariant derivative in the k -th sector with coupling $g^{(k)}$ and $F_{\mu\nu}^{(k)a} = \partial_{\mu} A_{\nu}^{(k)a} - \partial_{\nu} A_{\mu}^{(k)a} + g^{(k)} \varepsilon^{abc} A_{\mu}^{(k)b} A_{\nu}^{(k)c}$ is the k -th field strength. The potential is denoted by $V(\{|\phi|\})$.

This Lagrangian is invariant under the action of the product of N $SU_{(k)}(2)$ groups, in the form $SU_{(1)}(2) \times \dots \times SU_{(N)}(2)$. Each scalar field is a $SU(2)$ -valued quantity, given by $\phi^{(n)} = \phi^{(n)a} T^a$, where $T^a = -i\sigma^a/2$ are the generators of $SU(2)$, given in terms of the three Pauli matrices σ^a . Each $\phi^{(n)}$ is charged only in the respective $SU_{(n)}(2)$ subgroup, and is thus coupled to a gauge field $A_{\mu}^{(n)} = A_{\mu}^{(n)a} T^a$. The condition $\langle T^a, T^b \rangle = -2\text{Tr}(T^a T^b) = \delta^{ab}$ may be used to define an inner product in $SU(2)$, under which one obtains the norm $|\phi^{(n)}| = \sqrt{\phi^{(n)a} \phi^{(n)a}}$. Throughout this work, the Einstein summation convention is always implied for Lorentz and $SU(2)$ internal indices, but not for the remaining ones, which simply label the $SU(2)$ subgroups and are always enclosed in parentheses.

The functions $P^{(n)}$ and $M^{(n)}$ are nonnegative and may, in principle, depend on all the scalar fields $\{|\phi|\}$, respecting the gauge symmetry, but we shall shortly restrict their forms, aimed to implement some possibilities capable of giving interesting stable minimum energy configurations. We generically require that these functions take finite values when the field configurations approach the vacuum manifold, which will be topologically non trivial, in order to allow for finite energy topological solutions. The solutions can be classified according to a set of N integers, which, in analogy to the standard monopole, we may relate to quantized ‘‘magnetic’’ charges emerging from the unbroken $U(1)$ symmetry from each $SU(2)$ submanifold.

The field equations derived from (1) for the k -th sector

are

$$\begin{aligned} D_{\mu}^{(k)} \left(M^{(k)} D^{(k)\mu} \phi^{(k)a} \right) &= \frac{1}{4} \sum_{n=1}^N \frac{\partial P^{(n)}}{\partial \phi^{(k)a}} F_{\mu\nu}^{(n)b} F^{(n)b\mu\nu} \\ &+ \frac{1}{2} \sum_{n=1}^N \frac{\partial M^{(n)}}{\partial \phi^{(k)a}} D_{\mu}^{(n)} \phi^{(n)b} D^{(n)\mu} \phi^{(n)b} + \frac{\partial V}{\partial \phi^{(k)a}}, \end{aligned} \quad (2a)$$

$$D_{\mu}^{(k)} \left(P^{(k)} F^{(k)a\mu\nu} \right) = g^{(k)} M^{(k)} \varepsilon^{abc} \phi^{(k)b} D^{(k)\nu} \phi^{(k)c}, \quad (2b)$$

where the covariant derivatives also act in the following form $D_{\mu}^{(n)} F^{(n)a\mu\nu} = \partial_{\mu} F^{(n)a\mu\nu} + g^{(n)} \varepsilon^{abc} A_{\mu}^{(n)b} F^{(n)c\mu\nu}$.

Let us now consider static solutions, which may be obtained as time independent fields which obey equations of motion in a gauge such that $A_0^{(n)} = 0$ (leading to the non-abelian analogues of Gauss’ law to be trivially solved). The energy functional in this case is given by

$$\begin{aligned} E = \sum_{n=1}^N \int d^3x \left[\frac{1}{2} M^{(n)} |D_k^{(n)} \phi^{(n)}|^2 + \frac{1}{2} P^{(n)} |B_k^{(n)}|^2 \right. \\ \left. + V(\{|\phi|\}) \right], \end{aligned} \quad (3)$$

where $B_k^{(n)} \equiv \varepsilon_{ijk} F^{ij(n)}/2$ and the previously defined $su(2)$ norm has been used. We may now follow [6] to find a first order framework. This can be achieved by setting $M^{(n)} = 1/P^{(n)}$ for each n and taking the limit $V(\{|\phi|\}) \rightarrow 0$ in (3). This leads to

$$\begin{aligned} E = \sum_{n=1}^N \int d^3x P^{(n)} \left| B_k^{(n)} \pm \frac{D_k^{(n)} \phi^{(n)}}{P^{(n)}} \right|^2 \\ + 4\pi \sum_{n=1}^N \frac{v^{(n)}}{g^{(n)}} |Q_t^{(n)}|, \end{aligned} \quad (4)$$

where $Q_t^{(n)} \in \mathbb{Z}$ is the topological charge associated with the $(\phi^{(n)}, A_{\mu}^{(n)})$ solutions, defined in the same way as in the standard $SU(2)$ Yang-Mills-Higgs theory [9]. The second term in the right hand side is recognized as the summation of the fluxes arising from the magnetic fields in each sector. The observation that the first integral in (4) is non-negative leads to the Bogomol’nyi bound

$$E \geq 4\pi \sum_{n=1}^N \frac{v^{(n)}}{g^{(n)}} |Q_t^{(n)}|. \quad (5)$$

The equality in (5) is attained if and only if the first order equations

$$B_k^{(n)} = \mp \frac{D_k^{(n)} \phi^{(n)}}{P^{(n)}} \quad (6)$$

are satisfied for each n . By direct derivation it is straightforward to show that solutions of (6) always solve the second order equations. Deviations from the static case

give rise to quadratic terms in $F_{j0}^{(n)}$ and $\partial_0\phi^{(n)}$ which must be added to the integral in (3). Such terms may only increase the energy, and thus configurations that solve (6) are global minima of this functional.

We shall henceforth concern ourselves with spherically symmetric static solutions. Since we are choosing $A_0^{(n)} = 0$, as is well known, these restrictions allow us to write the fields in the form [3, 4]

$$\phi^{(n)a} = \frac{x_a}{r} H^{(n)}(r), \quad (7a)$$

$$A_i^{(n)a} = \varepsilon_{aib} \frac{x_b}{g^{(n)} r^2} (1 - K^{(n)}(r)), \quad (7b)$$

subject to the conditions

$$\begin{aligned} H^{(n)}(0) &= 0, & K^{(n)}(0) &= 1, \\ H^{(n)}(\infty) &\rightarrow \pm v^{(n)}, & K^{(n)}(\infty) &\rightarrow 0. \end{aligned} \quad (8)$$

These requirements ensure that the ensuing energy is finite, while also enforcing symmetry breaking and thus resulting in topological solutions. The form of this Ansatz implies $|Q_t^{(n)}| = 1$ for all n , so that the magnetic charge in each subsystem achieves the smallest non-zero value allowed by the quantization condition. Under these assumptions, the second order equations take the form

$$\begin{aligned} &\frac{1}{r^2} \left(r^2 M^{(n)} H^{(n)'} \right)' - \frac{2M^{(n)} H^{(n)} K^{(n)2}}{r^2} \\ &- \frac{1}{2} \sum_{k=1}^N \frac{\partial P^{(k)}}{\partial H^{(n)}} \left(\frac{2K^{(k)'}{}^2}{g^{(k)2} r^2} - \frac{(1 - K^{(k)2})^2}{g^{(k)2} r^4} \right) \\ &- \frac{1}{2} \sum_{k=1}^N \frac{\partial M^{(k)}}{\partial H^{(n)}} \left(H^{(k)'}{}^2 + \frac{2H^{(k)2} K^{(k)2}}{r^2} \right) \\ &- \frac{\partial V}{\partial H^{(n)}} = 0, \end{aligned} \quad (9a)$$

and

$$\begin{aligned} &r^2 \left(P^{(n)} K^{(n)'} \right)' - K^{(n)} \left\{ \left(M^{(n)} g^{(n)2} r^2 H^{(n)2} \right) \right. \\ &\left. + \left(P^{(n)} (1 - K^{(n)2}) \right) \right\} = 0, \end{aligned} \quad (9b)$$

where the prime denotes differentiation with respect to the radial coordinate. These equations constitute a set of $2N$ coupled and nonlinear ordinary differential equations. This system is very hard to solve, even when we choose simple couplings among the N sectors with $SU(2)$ symmetry to complete the model. For this reason, let us substitute the Ansatz into (6) and take the same assumptions used in that derivation to find the first order equations in the presence of spherical symmetry. For each n , there result two independent equations, obtained by projecting (6) into directions parallel and orthogonal to $\phi^{(n)}$, so that the energy is minimized by configurations that solve the N pairs of first order equations

$$H^{(n)'} = \pm P^{(n)} \frac{1 - K^{(n)2}}{g^{(n)} r^2}, \quad (10a)$$

$$K^{(n)'} = \mp g^{(n)} \frac{H^{(n)} K^{(n)}}{P^{(n)}}, \quad (10b)$$

for $n = 1, \dots, N$. These configurations saturate the Bogomol'nyi bound, with energy

$$E = 4\pi \sum_{k=1}^N \frac{v^{(k)}}{g^{(k)}}, \quad (11)$$

so that each $SU(2)$ subsystem contributes with an additive factor $4\pi v^{(k)}/g^{(k)}$ to the total energy. This, of course, is a reflection of the fact that these solutions have unity topological charges in each sector. We also note that the energy does not depend on any of the P^k , so the Bogomol'nyi bound only depends on the asymptotic values of the fields, which always approach the trivial vacuum solutions when the boundary conditions (8) are satisfied.

We may choose the functions P^k in a way that makes it easier to solve the first order equations while still keeping the subsystems coupled in a non-trivial way. In order to achieve this, we can consider several distinct possibilities, some of them will be considered below to illustrate the general situation. Before doing this, however, let us notice that the energy density for solutions of the first order equations can be written in the form

$$\rho(r) = \sum_{k=1}^N \rho^{(n)}(r), \quad (12)$$

where

$$\begin{aligned} \rho^{(n)}(r) &= \frac{2P^{(n)} K^{(n)'}{}^2}{(g^{(n)} r)^2} + \frac{H^{(n)'}{}^2}{P^{(n)}}, \\ &= \frac{P^{(n)} (1 - K^{(n)2})^2}{(g^{(n)} r^2)^2} + \frac{2(H^{(n)} K^{(n)})^2}{r^2 P^{(n)}}, \end{aligned} \quad (13)$$

which represents the energy density for the n -th sector.

III. MODELS WITH $N=3$

Let us first illustrate the aforementioned procedure with a few examples, in which the Lagrangian is of the form (1), with gauge group $SU(2) \times SU(2) \times SU(2)$. For simplicity, let us take $g^{(1)} = g^{(2)} = g^{(3)} = 1$ and $v^{(1)} = v^{(2)} = v^{(3)} = 1$ in our calculations and, since the upper and lower signs in equations (10) are related by changing $H \rightarrow -H$, we then only consider the upper signs in the investigation that follows.

A. First Model

As a first example, we shall consider a model with a standard monopole core, meaning $P^{(1)} = 1$. The $k = 1$ equations in (10) are thus

$$H^{(1)'} = \frac{1 - K^{(1)}}{r^2}, \quad (14a)$$

$$K^{(1)'} = -H^{(1)}K^{(1)}, \quad (14b)$$

which are simply the Bogomol'nyi equations for the 't Hooft-Polyakov monopole, for which an analytic solution has long been known [5]:

$$H^{(1)}(r) = \coth(r) - \frac{1}{r}, \quad K^{(1)}(r) = r \operatorname{csch}(r). \quad (15)$$

The energy density for this solution can be found from (13) to be

$$\rho_1(r) = \frac{[r^2 - \sinh^2(r)]^2}{r^4 \sinh^4(r)} + \frac{2(r \coth(r) - 1)^2}{r^2 \sinh^2(r)}. \quad (16)$$

We may now proceed as in [17] and introduce a shell structure by the choices $P^{(2)} = |\phi^{(1)}|^{-\alpha}$, $P^{(3)} = |\phi^{(2)}|^{-\beta}$, where α and β are positive integers. With these choices, we are led to the equations

$$H^{(2)'} = \left(\frac{1}{r \coth(r) - 1} \right)^\alpha \frac{1 - K^{(2)2}}{r^{2-\alpha}}, \quad (17a)$$

$$K^{(2)'} = -H^{(2)}K^{(2)} \left(\coth(r) - \frac{1}{r} \right)^\alpha. \quad (17b)$$

and

$$H^{(3)'} = \left(\frac{1}{H^{(2)}} \right)^\beta \frac{1 - K^{(3)2}}{r^2}, \quad (18a)$$

$$K^{(3)'} = -H^{(3)}K^{(3)} \left(H^{(2)} \right)^\beta. \quad (18b)$$

Note that we have inserted the solution (15) for $H^{(1)}(r)$ in equations (17), resulting in a system of two first order equations which can now be solved for the two unknown functions $H^{(2)}$ and $K^{(2)}$. We have not been able to obtain $H^{(2)}$ and $K^{(2)}$ in closed form, but the problem is amenable to numerical analysis. At large distances, $P^{(n)}(r) \rightarrow 1$ because of the boundary conditions, and we thus recover the asymptotic behavior of the standard solution. An analytical form can be obtained in a small neighborhood of the origin, where we have found $H^{(2)} = H_0^{(2)}$, $K^{(2)} = 1 - K_0^{(2)}$, with $H^{(2)} \propto r^{(-1-\alpha+\sqrt{\alpha^2+2\alpha+9})/2}$ and $K^{(2)} \propto r^{(1+\alpha+\sqrt{\alpha^2+2\alpha+9})/2}$. These expressions tell us how different choices of the parameter α may affect the short-distance behavior of the solution. A similar analysis can be conducted for the other shells and for every example we present here, but the explicit dependence on the radial coordinate becomes increasingly more complicated for the outermost shells, and shall therefore be omitted.

Once the full equations are solved numerically, we may plug the result $H^{(2)}$ in (18) in order to solve these equations. We have done this for the case $\alpha = 3, \beta = 10$, and present the results in FIGS 1, 2 and 3. One sees that in all cases these functions present a behavior that is qualitatively similar to that of the standard 't Hooft-Polyakov Monopole. The contributions ρ_1 , ρ_2 and ρ_3 to the energy density can be calculated from (13). Their behavior is represented in Figs. 1, 2 and 3. The last two contributions are strikingly different from the standard monopole solution (which has energy density equal to what we here have called ρ_1), presenting a maximum for $r \neq 0$.

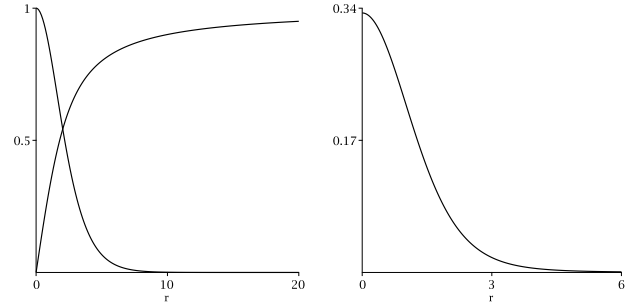


FIG. 1. In the left panel, we show the solutions $H^{(1)}(r)$ (ascending line) and $K^{(1)}(r)$ (descending line) of (14) for $\alpha = 3, \beta = 10$. Their analytical form is given by (15). In the right panel, we show the contribution ρ_1 to the energy density, given by (16).

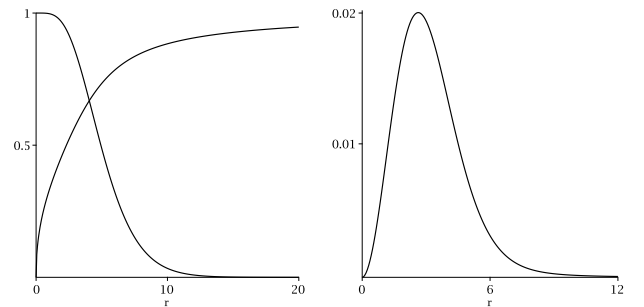


FIG. 2. In the left panel, we show the solutions $H^{(2)}(r)$ (ascending line) and $K^{(2)}(r)$ (descending line) of (17) for $\alpha = 3, \beta = 10$. In the right panel, we show the contribution ρ_2 , calculated from (13), relative to this sector.

The total energy could be calculated by direct integration of $\rho = \rho_1 + \rho_2 + \rho_3$, but these solutions solve the first order equations, so we may simply apply (11) to find $E = 12\pi$.

As a visual aid that may be useful for the interpretation of our results, we depict, in Fig. 4, a planar section of the energy density, in which the contributions ρ_1 , ρ_2 and ρ_3 have been plotted simultaneously. We see how a novel structure, comprised by a standard monopole core and two shells, arises from the superposition of the different subsystems. The size of each shell is controlled by the

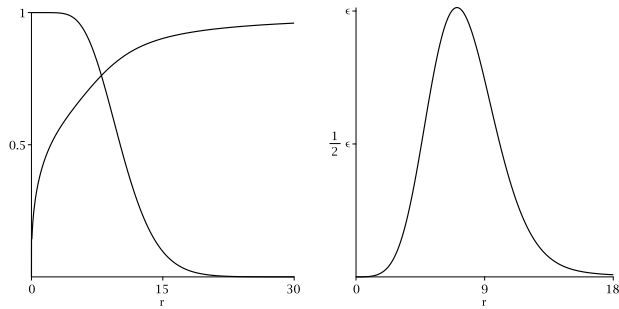


FIG. 3. In the left panel, we show the solutions $H^{(3)}(r)$ (ascending line) and $K^{(3)}(r)$ (descending line) of (18) for $\alpha = 3, \beta = 10$. In the right panel, we show the contribution ρ_3 , calculated from (13), relative to this sector. Here, $\epsilon = 0.0024$.

choice of the parameters α and β . The maxima of $\rho_1(r)$, $\rho_2(r)$ and $\rho_3(r)$ are attained at $r = 0$, $r \approx 2.6$ and $r \approx 7.1$, respectively.

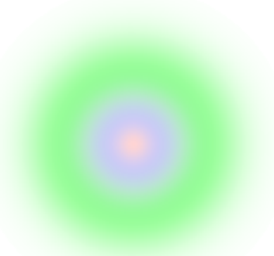


FIG. 4. Planar section, passing through the center, of the energy density, in which the contributions ρ_1 (red), ρ_2 (blue) and ρ_3 (green) calculated in subsection III A are shown, giving rise to a multimagnetic structure. We depict the case $\alpha = 3, \beta = 10$.

B. Second Model

As our second example, we abandon the standard core of the previous one, and take $P^{(1)} = |\phi^{(1)}|^{-\alpha}$, implying a self-interaction, as well as $P^{(2)} = |\phi^{(1)}|^{-\beta}$ and $P^{(3)} = |\phi^{(2)}|^{-\gamma}$. This combination of parameters will result in a triple shell structure, in which all three contributions to the energy density go to zero at the origin. In this example, the system of first order equations takes the form

$$H^{(1)'} = \left(\frac{1}{H^{(1)}}\right)^\alpha \frac{1 - K^{(1)2}}{r^2}, \quad (19a)$$

$$K^{(1)'} = -H^{(1)} K^{(1)} \left(H^{(1)}\right)^\alpha, \quad (19b)$$

and

$$H^{(2)'} = \left(\frac{1}{H^{(1)}}\right)^\beta \frac{1 - K^{(2)2}}{r^2}, \quad (20a)$$

$$K^{(2)'} = -H^{(2)} K^{(2)} \left(H^{(1)}\right)^\beta, \quad (20b)$$

and

$$H^{(3)'} = \left(\frac{1}{H^{(2)}}\right)^\gamma \frac{1 - K^{(3)2}}{r^2}, \quad (21a)$$

$$K^{(3)'} = -H^{(3)} K^{(3)} \left(H^{(2)}\right)^\gamma. \quad (21b)$$

Closed form solutions have not been discovered for any of the functions in this example, but we may solve these equations numerically. Once again, we find that the $H^{(n)}$ and $K^{(n)}$ present profiles that are qualitatively similar to those of the standard monopole solution. These solutions, as well as the individual contributions to the energy density, are represented in Figs. 5, 6 and 7. The total energy is again equal to 12π .

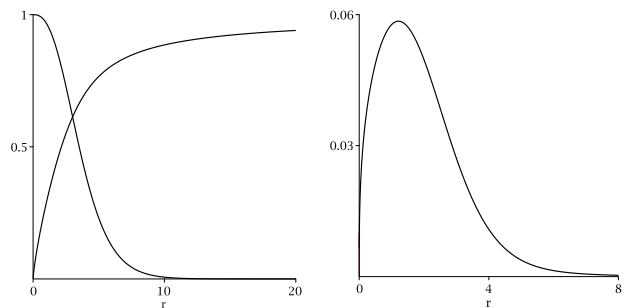


FIG. 5. In the left panel, we show the solutions $H^{(1)}(r)$ (ascending line) and $K^{(1)}(r)$ (descending line) of (19) for $\alpha = 1, \beta = 10$ and $\gamma = 30$. In the right panel, we show the contribution ρ_1 , calculated from (13), relative to this sector.

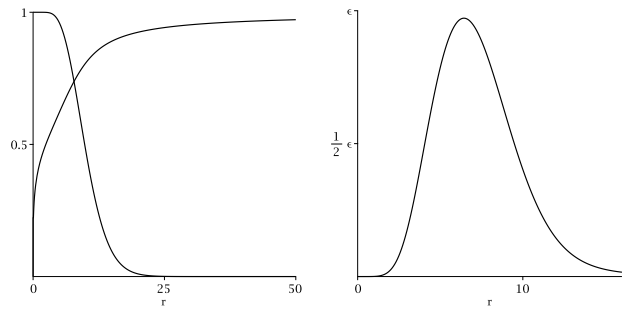


FIG. 6. In the left panel, we show the solutions $H^{(2)}(r)$ (ascending line) and $K^{(2)}(r)$ (descending line) of (20) for $\alpha = 1, \beta = 10$ and $\gamma = 30$. In the right panel, we show the contribution ρ_2 , calculated from (13), relative to this sector. Here we have $\epsilon = 0.0027$.

In Fig. 8, we show the densities ρ_1 , ρ_2 and ρ_3 simultaneously, which allows for visualization of the triple shell structure of this solution.

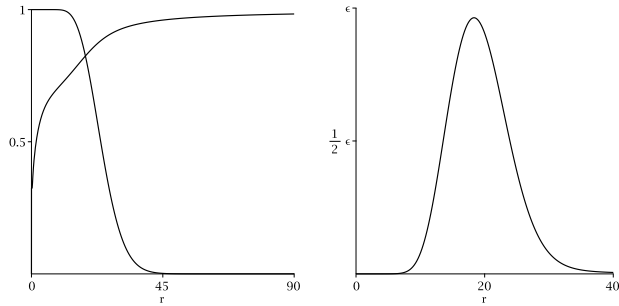


FIG. 7. In the left panel, we show the solutions $H^{(3)}(r)$ (ascending line) and $K^{(3)}(r)$ (descending line) of (21) for $\alpha = 1, \beta = 10$ and $\gamma = 30$. In the right panel, we show the contribution ρ_3 , calculated from (13), relative to this sector. Here, $\epsilon = 0.00022$.

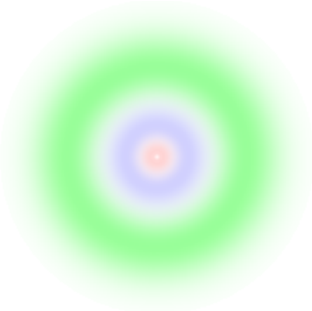


FIG. 8. Planar section, passing through the center, of the energy density, in which the contributions ρ_1 (red), ρ_2 (blue) and ρ_3 (green) calculated in subsection III B are shown, giving rise to a multimagnetic structure. We depict the case $\alpha = 1, \beta = 10, \gamma = 30$.

C. Third Model

We may also consider another possibility, which can be achieved by taking $P^{(2)}$ and $P^{(3)}$ as functions of $|\phi^{(1)}|$ alone. As an example, let us consider $P^{(1)} = 1, P^{(2)} = |\phi^{(1)}|^{-\alpha}$ and $P^{(3)} = |\phi^{(1)}|^{-\beta}$. This leads to equations (14) and (17), coupled to the additional pair of equations

$$H^{(3)'} = \left(\frac{1}{H^{(1)}} \right)^\beta \frac{1 - K^{(3)2}}{r^2}, \quad (22a)$$

$$K^{(3)'} = -H^{(3)} K^{(3)} \left(H^{(1)} \right)^\beta. \quad (22b)$$

This modification doesn't change the four other equations, the functions $H^{(1)}, K^{(1)}, H^{(2)}$ and $K^{(2)}$ are the same discussed in subsection III A. The substitution $H^{(1)}(r) = \coth(r) - 1/r$ in (22) gives rise to a system of ODEs that can be solved for $H^{(3)}$ and $K^{(3)}$. Their features are shown in Fig. 9, for $\beta = 12$. The multimagnetic structure that arises from the solution of the equations of motion is depicted in Fig. 10.

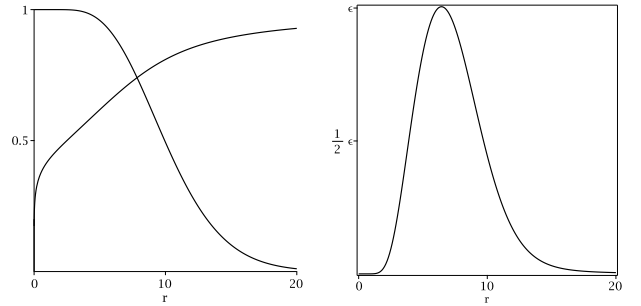


FIG. 9. In the left panel, we show the solutions $H^{(3)}(r)$ (ascending line) and $K^{(3)}(r)$ (descending line) of (22) for $\beta = 12$. In the right panel, we show the contribution ρ_3 , calculated from (13), relative to this sector. Here, $\epsilon = 0.0025$.

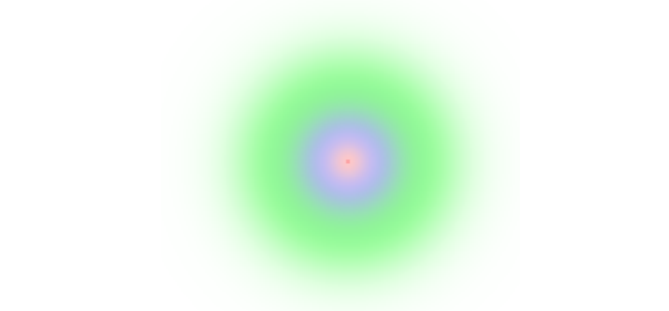


FIG. 10. Planar section, passing through the center, of the energy density, in which the contributions ρ_1 (red), ρ_2 (blue) and ρ_3 (green) calculated in subsection III C are shown, giving rise to a multimagnetic structure. We depict the case $\alpha = 3, \beta = 12$.

D. Fourth Model

As a final example of the $N = 3$ class of models, let us consider another example, in which $P^{(1)} = 1, P^{(2)} = |\phi^{(1)}|^{-\alpha}$ and $P^{(3)} = (|\phi^{(1)}||\phi^{(2)}|)^{-\beta}$. This model is different from the previous examples in that both the $\phi^{(1)}$ and $\phi^{(2)}$ fields appear explicitly in the third sector, with first order equations that are given by

$$H^{(3)'} = \left(\frac{1}{H^{(1)}H^{(2)}} \right)^\beta \frac{1 - K^{(3)2}}{r^2}, \quad (23a)$$

$$K^{(3)'} = -H^{(3)} K^{(3)} \left(H^{(1)}H^{(2)} \right)^\beta. \quad (23b)$$

These equations are coupled to (14) and (17), and we can plug in the results for $H^{(1)}$ and $H^{(2)}$ to solve (23). This has been done for the case $\alpha = 3, \beta = 10$. The solutions of (23) are displayed in Fig 11 and the multimagnetic structure associated to this case is shown in Fig 12.

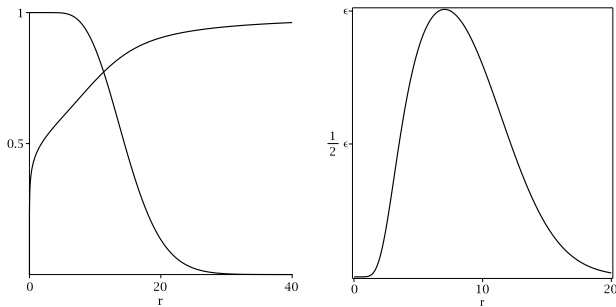


FIG. 11. In the left panel, we show the solutions $H^{(3)}(r)$ (ascending line) and $K^{(3)}(r)$ (descending line) of (23) for $\alpha = 3$, $\beta = 10$. In the right panel, we show the contribution ρ_3 , calculated from (13), relative to this sector. Here, $\epsilon = 0.0036$.

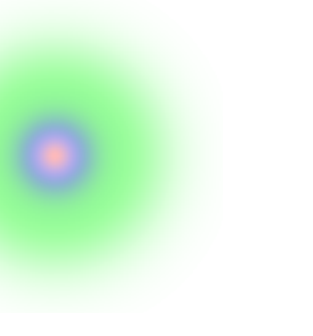


FIG. 12. Planar section, passing through the center, of the energy density, in which the contributions ρ_1 (red), ρ_2 (blue) and ρ_3 (green) calculated in subsection III D are shown, giving rise to a multimagnetic structure. We depict the case $\alpha = 3$, $\beta = 10$.

IV. MODELS WITH N=4

Let us now investigate another system, resulting in the group $SU(2) \times SU(2) \times SU(2) \times SU(2)$. This requires that we have four pairs of first order differential equations. The simplest way to achieve this is by adding a fourth pair of fields to the systems described in the previous section, and we investigate some distinct possibilities below.

A. First Model

As a first example, we take $P^{(1)}$, $P^{(2)}$ and $P^{(3)}$ as in our very first model of the previous Section and, additionally, choose $P^{(4)} = |\phi^{(3)}|^{-\gamma}$. We are then led to equations (14), (17) and (18), with the additional pair of first order equations

$$H^{(4)'} = \left(\frac{1}{H^{(3)}} \right)^\gamma \frac{1 - K^{(4)2}}{r^2}, \quad (24a)$$

$$K^{(4)'} = -H^{(4)} K^{(4)} \left(H^{(3)} \right)^\gamma. \quad (24b)$$

Since a solution for $H^{(3)}$ has already been found nu-

merically in subsection III A, we may plug this result in the equations above, and then solve them numerically. The result for the case $\alpha = 3$, $\beta = 10$, $\gamma = 20$, along with the contribution ρ_4 to the energy density, is shown in Fig. 13. We see that ρ_4 attains its maximum at $r \simeq 13.9$, and contributes to the energy with another 4π factor, raising its value to 16π .

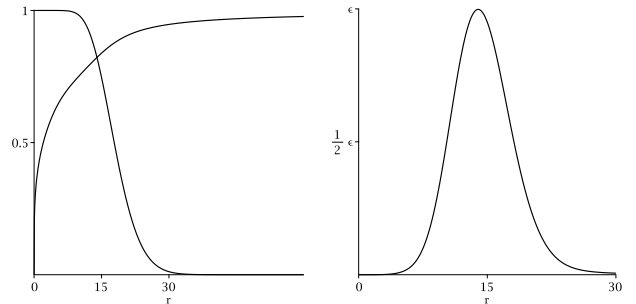


FIG. 13. In the left panel, we show the graph of the functions $H^{(4)}$ (ascending line) and $K^{(4)}$ (descending line) calculated from (24) which, together with the functions obtained in subsection III A, form a solution of the equations of motion. In the right panel, we show the contribution ρ_4 , calculated from (13), relative to this sector. Both plots correspond to the choices $\alpha = 3$, $\beta = 10$, $\gamma = 20$ of the model's parameters. Here, $\epsilon = 0.0005$.

Moreover, we depict in Fig. 14 the multimagnetic structure which results from the superposition of the four subsystems considered.



FIG. 14. Planar section, passing through the center, of the four contributions ρ_1 (red), ρ_2 (blue), ρ_3 (green) and ρ_4 (black) relative to the model presented in subsection IV A for $\alpha = 3$, $\beta = 10$, $\gamma = 20$.

B. Second Model

As another example, we present a solution with four shells. To achieve this, we take P^1 , P^2 and P^3 as in subsection IV A, as well as $P^{(4)} = |\phi^{(3)}|^{-\zeta}$. This case results in a system of equations comprised by (19), (20)

and (21), which are now coupled with the additional pair of equations

$$H^{(4)'} = \left(\frac{1}{H^{(3)}} \right)^\zeta \frac{1 - K^{(4)2}}{r^2}, \quad (25a)$$

$$K^{(4)'} = -H^{(4)} K^{(3)} \left(H^{(3)} \right)^\zeta. \quad (25b)$$

The equations have again been solved through numerical procedures, and the results can be seen in Fig. 15 below. The energy density $\rho_4(r)$ has a peak at $r \approx 8.2$. We then present in Fig. 16 the multimagnetic structure that arises from the superposition of the four subsystems considered.

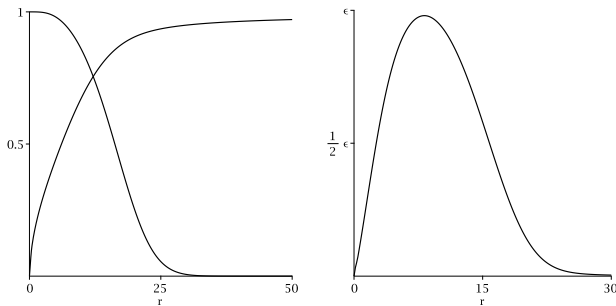


FIG. 15. In the left panel, we show the graph of the functions $H^{(4)}$ and $K^{(4)}$ which solve (25) and, together with the functions calculated in subsection III B, form a solution of the equations of motion. In the right panel, we show the contribution ρ_4 to the energy density. Both plots correspond to the choices $\alpha = 1$, $\beta = 10$, $\gamma = 30$, $\zeta = 8$ of the model's parameters. Here, $\epsilon = 0.0006$.



FIG. 16. Planar section, passing through the center, of the four contributions ρ_1 (red), ρ_2 (blue), ρ_3 (yellow) and ρ_4 (green) to the energy density relative to the model presented in subsection IV B for $\alpha = 1$, $\beta = 10$, $\gamma = 30$, $\zeta = 8$.

In the case with $N = 4$ there are several other possibilities, similar to the case of $N = 3$ which we have investigated above.

V. DISCUSSION

In this work we studied the presence of magnetic monopoles in a relativistic model with a modified Lagrangian that is invariant under N copies of the $SU(2)$ symmetry, that is, $SU_{(1)}(2) \times SU_{(2)}(2) \times \dots \times SU_{(N)}(2)$. We presented a general investigation leading to the presence of first order differential equations that solve the equations of motion and ensure the presence of minimum energy configurations. We then discussed some examples with $N = 3$ and $N = 4$, with shells on top of a standard monopole core and in other cases, giving rise to novel onionlike structures. We believe that these multimagnetic structures may find applications several areas of nonlinear science. In particular, the solutions generalize the bimagnetic structures considered before in [17], and they may find applications in several different scenarios in condensed matter [19, 20, 29, 32].

It is worthwhile to notice that instead of the replication of the $SU(2)$ symmetry, we could also chose other models with gauge groups of the form $G_1 \times \dots \times G_N$, where the G_k are themselves non-abelian gauge groups. One particularly interesting example is found for the gauge group $SO(10)$. This particular grand unification theory has been studied for quite some time [33, 34] and is considered a relatively simple and promising unification model [35, 36]. This gauge group may undertake symmetry breaking to $SU(3) \times SU(2) \times SU(2) \times U(1)$ as an intermediary step before reduction to the gauge group of the standard model [37]. Thus, we could take, for example, an $SU(3)$ core with two shells provided by the symmetry breaking from the $SU(2) \times SU(2)$ subgroup. Although mathematically more challenging, this case is, in principle, a straightforward extension of the examples provided here. In the same way, we could also consider the $SU(3)$ and $SU(5)$ gauge groups, since they also support monopoles [38, 39] and may be used with distinct motivations. Another line of current interest concerns the study of the magnetic monopoles found in the present work interacting with gravity, to see how they change the standard scenario of black holes in magnetic monopoles [40]. As we can see, the underlying principle leading to the solutions studied in this work may lead to a wide range of multimagnetic monopoles, differing by the gauge group and by the many possible choices for the functions that modify the standard model. We hope that the above results will foster new investigation on magnetic monopoles.

ACKNOWLEDGMENTS

The work is supported by the Brazilian agencies Coordenação de Aperfeiçoamento de Pessoal de Nível Superior (CAPES), grant No 88887.485504/2020-00 (MAL), Conselho Nacional de Desenvolvimento Científico e Tecnológico (CNPq), grants No. 303469/2019-6 (DB) and No. 404913/2018-0 (DB), and by Paraíba State Research Foundation (FAPESQ-PB) grant No. 0015/2019.

-
- [1] P. A. M. Dirac, Proc. R. Soc. Lond. A 133, 60 (1931).
- [2] P. A. M. Dirac, Phys. Rev. 74, 817 (1948).
- [3] G. 't Hooft, Nucl. Phys. B 79, 276 (1974).
- [4] A. M. Polyakov, JETP Lett. 20, 194 (1974).
- [5] M. K. Prasad and C. M. Sommerfield, Phys. Rev. Lett. 35, 760 (1975).
- [6] E. B. Bogomol'nyi, Sov. J. Nucl. Phys. 24, 449 (1976).
- [7] J. Arafune, P. G. O. Freund, and C. J. Goebel, J. Math Phys. 16, 433 (1975).
- [8] P. Rossi, Phys. Reports 86, 317 (1982).
- [9] N. Manton and P. Sutcliffe, *Topological Solitons*, Cambridge University Press (2004).
- [10] B. M. Einhorn, D. L. Stein, Phys. Rev. D 21, 3295 (1980).
- [11] A. H. Guth, Phys. Rev. D 23, 347 (1981).
- [12] K. A. Olive, D. Seckel, *Primordial Inflation and the Monopole Problem*, J.L. Stone (eds), Monopole 83 111, Springer (1984).
- [13] E. Witten, Nucl. Phys. B 249, 557 (1985).
- [14] M. Shifman, Phys. Rev. D 87, 025025 (2013).
- [15] D. Bazeia, M. A. Marques, and R. Menezes, Phys. Rev. D 97, 105024 (2018).
- [16] D. Bazeia, M. $i_{\frac{1}{2}}i_{\frac{1}{2}}$ A. Marques, and Gonzalo J. Olmo, Phys. Rev. D 98, 025017 (2018).
- [17] D. Bazeia, M. A. Marques, and R. Menezes, Phys. Rev. D 98, 065003 (2018).
- [18] D. Bazeia, M. A. Liao, M. A. Marques, and R. Menezes Phys. Rev. Research 1, 033053 (2019).
- [19] M. Estrader et al., Nat. Commun. 4, 2960 (2013).
- [20] A. López-Ortega, M. Estrader, G. Salazar-Alvarez, A. G. Roca, and J. Nogués, Phys. Rep. 553, 1 (2015).
- [21] I. Groza, R. Morel, A. Brenac, C. Beigne, C. and L. Notin IEEE Trans. Magn. 47, 3355 (2011).
- [22] J.-H. Lee, J.-T. Jang, J.-S. Choi, S. H. Moon, S.-H. Noh, J.-W. Kim, J.-G. Kim, I.-S. Kim, K. I. Park, and J. Cheon, Nat. Nanotechnol. 6, 418 (2011).
- [23] V. Skumryev, S. Stoyanov, Y. Zhang, G. Hadjipanayis, D. Givord and J. Nogués, Nature, 423, 850 (2003).
- [24] R. F. L. Evans, R. Yanes, O. Mryasov, R. W. Chantrell and O. Chubykalo-Fesenko, EPL, 88, 57004 (2009).
- [25] G. Salazar-Alvarez et al., J. Am. Chem. Soc. 133, 16738 (2011).
- [26] L. Catala, D. Brinzei, Y. Prado, A. Gloter, O. Stéphan, G. Rogez and T. Mallah, Angew. Chem., Int. Ed. 48, 183 (2008).
- [27] C. Castelnovo, R. Moessner, and S. L. Sondhi, Nature 451, 42 (2008).
- [28] T. Fennell et al., Science 326, 415 (2009).
- [29] N. Kanazawa et al., Phys. Rev. Lett. 125, 137202 (2020).
- [30] O. Gould and A. Rajantie, Phys. Rev. Lett. 119, 241601 (2017).
- [31] B. Acharya et al. Int. J. Mod. Phys. A 29, 1430050 (2014).
- [32] F.A. Cardona et al., RSC Adv. 6, 77558 (2016).
- [33] H. Fritzsche and P. Minkowski, Ann. Phys. (N.Y.) 93, 193 (1975).
- [34] H. Georgi, AIP Conf. Proc. 23, 575 (1975).
- [35] T. Fukuyama, Int. J. Mod. Phys. A 28, 1330008 (2013).
- [36] G. G. Ross, *Grand Unified Theories* (Addison-Wesley, 1985).
- [37] F.F. Deppisch, T.E. Gonzalo and L. Graf, Phys. Rev. D 96, 055003 (2017).
- [38] P. Irwin, Phys. Rev. D 56, 5200 (1997).
- [39] L. Pogosian, D. A. Steer, and T. Vachaspaty, Phys. Rev. Lett. 90, 061801 (2003).
- [40] K. Lee, V. P. Nair, and E. J. Weinberg, Phys. Rev. D 45, 2751 (1992).